THE SPATIAL LAG EFFECTS OF BED LOAD TRANSPORT UNDER UNSTEADY FLOW CONDITIONS

Arie Setiadi Moerwanto

Pusat Penelitian dan Pengembangan Sumber Daya Air
Jl. H. Juanda no. 193, Bandung
E-Mail: ariemoerwanto@yahoo.com

Diterima: 25 Agustus 2010 ;Disetujui: 29 Oktober 2010

ABSTRAK

Peningkatan kecepatan pengolahan dan kapasitas penyimpanan data acak pada komputer pribadi memberikan peluang dan tantangan dalam pengembangan pemodelan numerik respon morfologi sungai pada kondisi aliran langgeng maupun tidak, berbasis metode penyelesaian elemen hingga. Sebagai konsekuensi, efek-efek kelambanan spasial dan temporal akibat perubahan tiba-tiba kondisi hidrodinamika aliran sungai maupun persyaratan pengambilan jenjangan spasial numerik yang lebih pendek daripada panjang ruas sungai yang diperlukan oleh sistem aluvial untuk beradaptasi terhadap perubahan kondisi hidrodinamika aliran harus benar-benar diperhitungkan dengan baik. Dalam tulisan ini dibahas secara rinci cara pemodelan, termasuk pengujian unjuk kerja model dalam menirukan khususnya efek kelambanan spasial sistem aluvial.

Kata kunci: *Efek kelambanan spasial, metode elemen hingga, unjuk kerja model.*

ABSTRACT

The recent rapid development on the computation speed and capacity of random access memory of personal computer has presented opportunities and challenges on the implementation of finite element method on the modelling of river morphology response under steady as well as unsteady flow conditions. As consequences, the temporal and spatial lag effects due to sudden changes in hydrodynamic conditions as well as the requirement to take numerical space steps that are shorter than the adaptation length of the alluvial system to adjust to the changes in hydrodynamic conditions must be well taken into account. This paper describes in detail the modelling method including testing of model performance in simulating particularly the spatial lag of alluvial system.

Keyword: *Spatial lag effect, finite element method, model performance.*

INTRODUCTION

The spatial lag of bed load transport is the inability of the flow over an alluvial bed to directly reach its new bed load transport capacity due to sudden changes in either the bed load transport capacity or the sediment availability. As an example, this phenomenon occurs in a system which consists of a steady uniform flow over a non-erodible reach at the upstream end followed by an alluvial reach at the downstream end. These phenomena are normally faced in the cases of released water from spillway of dams and weirs or hydropower plants.

As the clear water flow proceeds from the non-erodible bed to the moveable bed, the flow will entrain sediment particles from the bed to begin satisfying its transport capacity. This process will require a passage over a finite length of erodible bed to overcome the non-equilibrium of sediment transport. The deficit in sediment transport decreases in the downstream direction until the bed load sediment transport capacity is reached. The required distance to reach the transport capacity is termed as the adaptation length of bed load transport. The spatial lag effects of bed load transport can also take place when there is any sudden change in the cross-sectional flow area, whether it be a widening or narrowing, a deepening or swallowing of the flow.

The spatial lag phenomenon of the bed load transport that should be taken into account and the techniques used to incorporate it in a numerical model of river morphology changes are discussed in the present study. Adopting the spatial lag phenomenon allows the model to be run under unsteady flow conditions and taking

unequal grids or space steps required to have detailed specific field conditions.

This study is being carried under a scheme of the development of A Riverine Fully Coupled Finite Element Model with Sediment Transport Sub-processes as a required tool to support the adaptation policy to respond to the global climate change.

AIMS

To simulate spatial lag effects of alluvial system under steady as well as unsteady flow conditions using finite element method.

To adequately represent the river morphological changes, it is desirable to develop a one-dimensional numerical morphological model of rivers that has capabilities of simulating various sediment transport sub-processes and been setup by considering the following aspects:

1) the adoption of the dynamic wave approach by retaining all the terms in the momentum equation,
2) the explicit separation of the bed load and the suspended load transport,
3) the vertical exchange of sediment and armored layer development and a means of handling non-uniform distribution of bed material, and
4) incorporating the spatial and temporal lag effects of bed load transport as a consequence of the dynamic wave approach.

Under that mentioned frameworks, the particular aims of the present study are to find a method of simulating the spatial effect of bed load transport, coding it with finite element solution and to verify its performances. The inclusion of this phenomenon will allow the model to cope with the following conditions:

1) an imposed of non-equilibrium sediment boundary condition,
2) situations where the space steps need to be taken shorter than the adaptation length required by the flow to reach its transport capacity, and
3) condition where the actual sediment transport rate is different from the flow transport capacity.

LITERATURES REVIEW

The earlier research which describes the spatial lag of bed load transport is the research on the pickup rate of bed particles (Einstein, 1950; Yalin, 1977; van Rijn, 1984b; Singh, 2004). Intensive flume experimentation on the spatial lag of bed load transport, was undertaken by Bell (Bell, 1980; Bell and Sutherland, 1983). Bell conducted his experiments in the partly moveable bed flume which consisted of a rigid bed for the upstream reach followed by a reach of moveable bed. The experiment started by establishing steady flow conditions and an equilibrium bed load transport. For this purpose, sediment was supplied by means of a sediment vibrating hopper at the upstream end of the flume. Later, the sediment supply was stopped, creating a non-equilibrium bed load transport while the steady flow was preserved. Based on the measured space variation of the bed load transport rate downstream of the rigid bed, the following relation was proposed to represent the spatial lag of the bed load transport (Bell, 1980; Bell and Sutherland, 1983):

$$\frac{\partial Q_{sb_j}}{\partial x} = C_{SL_j}\left(Q^e_{sb_j} - Q_{sb_j}\right) + \frac{Q_{sb_j}}{Q^e_{sb_j}}\frac{\partial Q^e_{sb_j}}{\partial x} \quad \text{... (1)}$$

where

C_{SL_j}, spatial lag coefficient of bed load transport for the j^{th} sediment size class, [m^{-1}];

Q_{sb_j}, volumetric transport of bed load sediment for the j^{th} sediment size class, [m^3/s];

$Q^e_{sb_j}$, volumetric transport capacity of bed load sediment for the j^{th} sediment size class,[m^3/s].

The spatial lag coefficient of bed load transport C_{SL_j} depends on the local hydraulic conditions. Phillips (1984 and 1989) proposed the following empirical relation for the spatial lag coefficient in the specified range for α_L :

$$C_{SL_j} = \frac{1}{\alpha_L\left(\theta_j - \theta_{cr_j}\right)D_j}$$

for $4000 \le \alpha_L \le 9000$ **(2)**

where

α_L , Yalin's step length parameter, [-];

θ_j , $\frac{u_*^2}{\Delta g D_j}$, dimensionless Shields parameter for the j^{th} sediment size class;

θ_{cr_j} , $\frac{u_{cr}^{*2}}{\Delta g D_j}$, dimensionless critical Shields parameter for the j^{th} sediment size class.

No definite value is proposed for the parameter α_L. However, tests carried out in the

present study show that the model results are not sensitive to the selected Yalin's step length parameter α_L. Equations **(1)** and **(2)** are adopted and explored its robustness in the present developed numerical model to represent the spatial lag effects of bed load transport.

To cope with these problems when non-equilibrium bed load transport is imposed at the upstream boundary, a dummy space step is normally added to the upstream end of the simulated channel. The dummy space step is used to adapt the imposed non-equilibrium bed load transport to the bed load transport capacity of the flow. In contrast, the adoption of Equations **(1)** and **(2)** enables the present model to simulate a condition where the non-equilibrium bed load transport is imposed at the upstream boundary without adding the dummy space steps.

METHODOLOGY

This present study is carried out to support the development of A Riverine Fully Coupled Finite Element Model with sediment transport sub-processes. To achieve an efficient and robust sub-model that could easily communicate with the main model, the structure of Bed-load Sediment Transport Sub-model is also designed by implementing the modularity advantages of finite element solution. The performances of the sub-model are steps by steps verified by comparing its prediction results with set of data resulted from physical hydraulic laboratory tests.

1 Setting Up of Bed Load Sediment Transport Sub-Model

To achieve the desirable model, the following two field phenomena of bed load transport are incorporated and simulated by the bed load transport sub-model:

1) The bed load sediment transport capacity under unsteady flows is analyzed by including the temporal lag effects of the alluvial reach.
2) The actual bed load sediment transport rate is analyzed by including the spatial lag effects of the bed load transport as formulated in Equations (1) and (2).

The structure diagram of the designed bed load transport sub-model as a subroutine of the developed riverine fully coupled finite element model is shown in Figure 1.

2 Test on Simulating Local Scouring Downstream of a Sediment Barrier

Non-steady hydrodynamics can cause transients in the bed of alluvial channels. Nevertheless, a change in the upstream sediment transport supply under steady hydrodynamic conditions will also generate morphological transients. A series of tests is performed to assess the capability of the sub model to simulate the spatial lag effect and the time variation of the bed load transport rate, and the mean bed elevation within a region affected by an imposed non-equilibrium boundary condition. For this purpose as presented in Figure 3, flume experiments conducted by Bell (1980 and 1983) on non-equilibrium bed load transport downstream of a horizontal, roughened, fixed bed are simulated.

1) Experimental equipment and procedure

Bell (1980 and 1983) conducted the experiment on an open circuit tilting flume with: length, L = 30.0 m, width, B = 0.305 m and initial bed slope, I_0 = 0.002. The other data was as follows:

1) To fully develop the turbulent boundary layer before reaching the erodible bed, a fixed roughened bed was set up at upstream section of the flume.
2) The erodible bed material consisted of uniform fine gravel particles of mean diameter D_m = 2.11 mm and geometric standard deviation σ_g = 1.25.

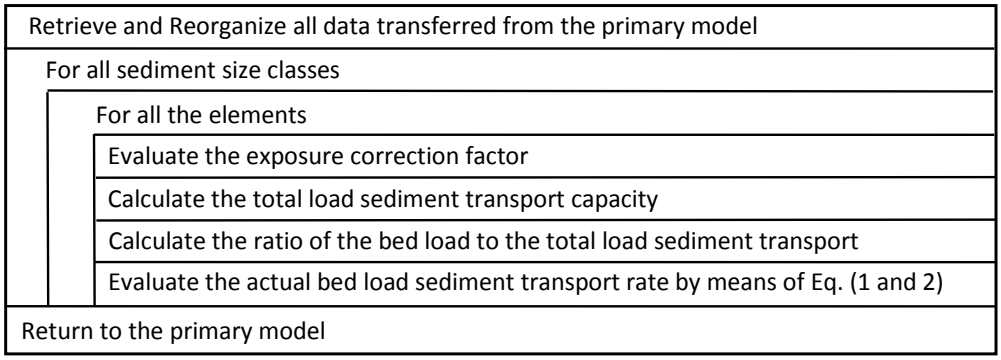

Figure 1 Structure diagram of the bed load sediment transport sub-model

3) The depth was adjusted by means of a submerged weir which was placed at the downstream end of the flume.
4) A bed load collector, that could be lowered to follow the degrading bed level, was setup to collect the eroded sediment.

In the flume experiments, steady flow conditions and equilibrium sediment transport were first established. For this purpose, sediment was supplied to the system at the upstream end of the test reach from a vibrating hopper at a prescribed rate. Later the sediment supply at the upstream boundary was stopped. Using this procedure, non-equilibrium sediment transport conditions were generated without creating unsteady water flow conditions.

2) Model Simulation

a) Schematization of the flume experiments

The first part of the flume was designed to direct the flow in such a way that the incoming flow is parallel to flume walls and to give rise to a fully developed turbulent boundary layer in the approach flow. Since the numerical model is one dimensional, it is the flume for the simulation. Moreover, the simulations are carried out by using the following setup:

1) The first node of the numerical model is at the downstream end of the fixed, roughened bed, while the last node is placed 100 m downstream of this node.
2) This 100 m long reach is divided into 24 non-uniform elements, with space steps starting at 0.25 m for the upstream elements and gradually enlarged up to 20 m for the downstream elements.

The chainage along flume and the layout of the nodes in the linear finite elements are presented in Figure 2.

b) Initial conditions and upstream boundary conditions

Bell (1980) noted that all sediment particles were transported as bed load. Therefore, the advection-dispersion equation for the suspended load transport can be omitted and the primary variables in these experiments are: the discharge, Q; the surface water elevation, z; the bed level, z_b; the bed load transport rate Q_{sb} and inflow discharge per unit width of q = 0.159 $m^3/s/m$. Each primary variable must be specified at all nodes at time t = 0 for the initial conditions. In the present case, the initial conditions applied are steady flow, ie. hydrodynamics, and equilibrium bed load transport rates.

c) Upstream boundary conditions

The imposed upstream boundary conditions in the numerical simulations are:

1) One primary variable related to the bed load transport is required at the upstream boundary to solve the sediment mass balance equation.
2) The locally scoured bed material due to a fluid vortex is chosen for this purpose. Detailed setup of this upstream boundary is discussed in Sub-section 3.

d) Downstream boundary

In the flume experiments, the downstream water surface elevation was kept constant during each experiment by means of a fully sub merged weir. The weir was located in the non-erodible reach downstream of the bed load collector,

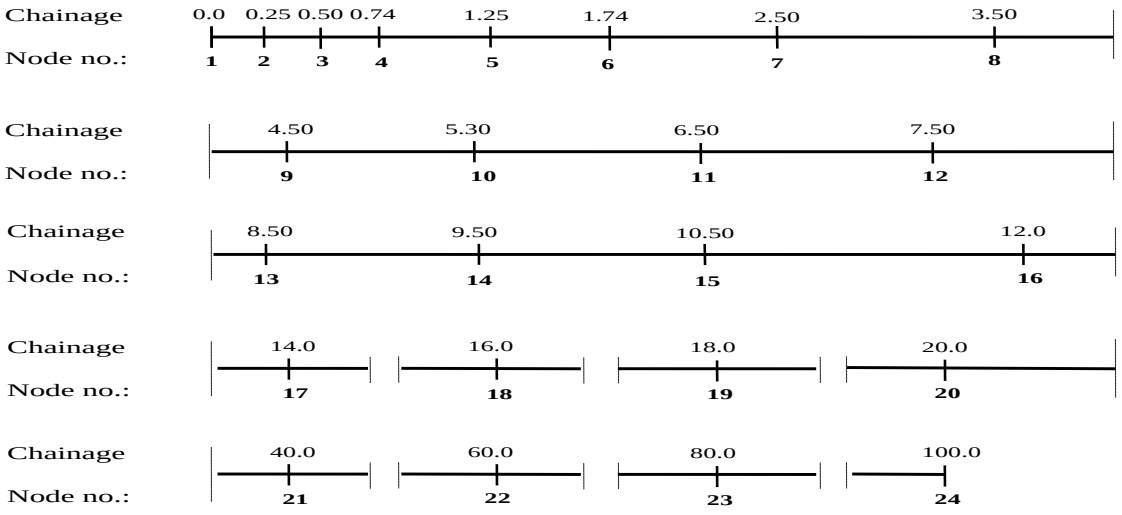

Figure 2 Chainage along the flume and element configuration of the numerical model

which means that no bed level change occurred in just upstream of the weir. To simulate this condition, a longer reach than was simulated in the flume is used. This avoided bed disturbances reaching the downstream boundary. A constant surface water elevation is setup at the downstream boundary for each time step.

e) Bed load transport formula

A relation for the bed load transport capacity proposed by Phillips (1984) is used in these model tests. The relation developed by Phillips based on flume data of Bell (1980) for steady flow conditions and uniform bed material is as follows:

$$Q_{sb}^{e} = 1.032 \frac{\left(u - u_{cr}\right)^{2.52}}{\rho_s} B_{act} \quad \text{... (3)}$$

where

B_{act}, the active portion of channel bed width in which erosion and deposition takes place, [m];

Q_{sb}^{e}, volumetric transport capacity of bed load sediment, [m^3/s];

u, flow velocity in the channel, [m/s];

u_{cr}, critical flow velocity for the initiation of sediment particle motion, [m/s];

ρ_s, mass density of sediment, [kg/m^3].

f) Bed roughness coefficient

The presence of a scour hole and bed forms will influence the effective bed roughness. To accommodate these effects, a method based on integral parameters was proposed by Bell (1980) to estimate the effective bed roughness of the simulated flume conditions. The aforementioned relation for Manning's bed roughness coefficient, which is used in the model tests, is as follows:

$$n = 0.0256\,\theta^{0.136} \quad \text{...(4)}$$

where

n, Manning coefficient, [m$^{-\frac{1}{3}}$/s];

θ, dimensionless Shields parameter.

g) Side wall correction for bed shear stress

In flume experiments, the surfaces of the side walls will normally be smoother than an alluvial bed and this causes a non-uniform distribution of boundary shear stress. As the bed becomes rougher or the flow depth decreases, the wall shear stress decreases relative to the bed shear stress. A side wall roughness correction is needed in order to standardize the flume results. The same correction is required when the relations developed for field conditions are implemented in the flume conditions. In applying the side wall roughness correction, the total shear stress is separated into the components of bed shear stress and wall shear stress. The method is based on the Darcy-Weisbach formula (Johnson, 1942). Later, this method was modified and simplified by providing a simple graphical solution for side wall roughness correction (Vanoni and Brooks, 1957). A simple empirical side wall roughness correction was proposed by Williams (Bell, 1983). In this method, the laboratory values of slope and shear stress were converted into equivalent wide channel values for the same flow depth and unit transport of sediment. Bell (1983) analyzed his flume results and came to a conclusion that the method of Williams gave the best fit to his data. Based on this conclusion, Bell used the Williams method to standardize his flume results. Hence, the method of Williams for side wall roughness correction is also adopted in the present model tests. Using the side wall roughness correction of Williams, the bed shear velocity, u_{*_b}, is given by:

$$u_{*_b} = \frac{u_*}{\sqrt{1.0 + 0.055\,\frac{h}{B^2}}} \quad \text{...(5)}$$

where

$$u_* = \sqrt{g.h.I_f} \quad \text{...(6)}$$

$$u_{*_b} = \sqrt{g.R_b.I_f} \quad \text{...(7)}$$

and

B, flume width, [m];

R_b, hydraulic radius of the bed defined to analyze the flume bed shear stress, [m];

I_f, friction slope, [-];

h, averaged flow depth, [m].

Substituting equations **(6)** and **(7)** into equation **(5)** results in:

$$R_b = \frac{h}{1.0 + 0.055\,\frac{h}{B^2}} \quad \text{...(8)}$$

This corrected hydraulic radius of the flume bed is used in the present model tests to analyze bed shear stress, bed roughness and bed load transport.

3) Incorporating the locally scoured bed material into the upstream boundary

In a case where there is no sediment input, the moveable bed downstream of a fixed bed is scoured, a zone of separation occurs and a fluid vortex forms (Figure 3). The scour hole deepens under this fluid vortex until it reaches a local maximum depth at the downstream extremity of the vortex (Breusers, 1965; Bell, 1980; Phillips, 1984 and Yiniarti, 2008). These processes refer to the local scouring. This locally scoured bed material influences the bed load sediment transport rate and requires to be taken into account in the sediment mass balance equation. Therefore in the present model, the locally scoured bed material is bounded in the upstream boundary for the sediment module. Furthermore, this upstream boundary is located at the point of local maximum scour.

Since the location of the maximum local scour moves downstream with time, the location of the upstream sediment boundary does likewise and results in a mobile boundary condition. To model this condition, the location of the point of local maximum scour and the volume of scoured bed material at each time step are required.

Based on measured data of Breusers (1965) presented in Figure 4, the following cubic equation of best fit to typical scour hole profiles in the zone of separation was proposed by Phillips (1984):

$$\frac{z_{bs}}{z_{bs_{\max}}} = 1.5\left(\frac{x}{L}\right)^3 - 4.0\left(\frac{x}{L}\right)^2 + 3.5\left(\frac{x}{L}\right) \quad \text{... (9)}$$

where

z_{bs}, scour depth measured from the plane bed at $t = 0$, [m];

L, distance to the point of local maximum scour from the edge of fixed bed, [m];

$z_{bs_{\max}}$, local maximum scour depth, [m].

Further relation are required to determine L and z_{bs}. Based on the flume data of Bell (1980), Phillips proposed the following relations:

$$\frac{L}{z_{bs_{\max}}} = 65.5\varepsilon^{-0.5094} \quad for \quad \varepsilon \le 150$$

$$\frac{L}{z_{bs_{\max}}} = 5.1 \quad for \quad \varepsilon > 150 \quad \text{... (10)}$$

where

ε, $\dfrac{u_1 - u_{cr_1}}{w} D_{gr}$

D_{gr}, dimensionless grain size, (-),

$D\left(\dfrac{\Delta g}{\nu^2}\right)^{\frac{1}{3}}$,

u_1, flow velocity at the downstream end of the fixed bed, [m/s];

u_{cr_1}, critical flow velocity for the initiation of sediment movement at the downstream end of the fixed bed, [m/s];

w, sediment fall velocity, [m/s].

The movement of the point of local maximum scour is demonstrated in Figure 5. During a time step, Δt, the location of the point of local maximum scour moves from point **A** in Section 2 to point **B** in Section 3. At any given time, the upstream boundary scheme predicts the

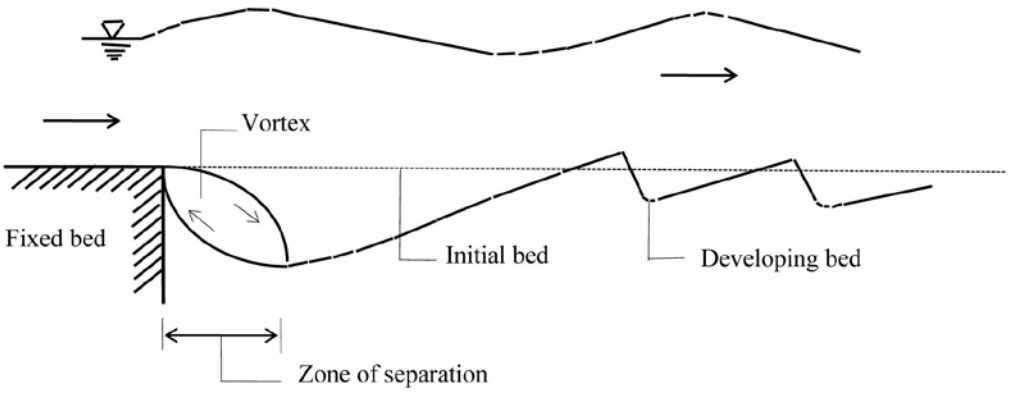

Figure 3 Flow field in a local scour hole downstream of a fixed bed

location of Section 3 and calculates the sediment transport rate at the new time level at this section. At the end of any time level, $t + \Delta t$, the volumetric bed load transport rate is given by:

$$Q_{sb}^{(t+\Delta t)} = \frac{(1-p).B_{act}.\Delta V_b}{\Delta t} \quad \text{... (11)}$$

where

ΔV_b, volume of the scoured bed per unit width of the active portion of channel bed over the time step, [m^2].

Integration of equation **(9)** for a typical scour hole profile results in a total volume of scour per unit width of the active portion of channel bed as follows:

$$V_b = 0.791\, z_{bs}.L \quad \text{... (12)}$$

From the scour hole profiles at time levels t and $t + \Delta t$ in Figure 5, the volume of bed scoured in Δt is:

$$\Delta V_b = 0.791\, L_3.(z_{bs})_3 - 0.791\, L_2.(z_{bs})_2 - (L_3 - L_2).(z_{bs})_2 \quad (13)$$

Sediment free water entering section 1 scours the moveable bed and results in a bed load transport rate at Section 3. This bed load transport rate, which is evaluated by using equations **(9)** to **(13)**, is used as the upstream sediment boundary condition for the numerical model.

4) Scenarios of the carried out model tests

As discussed earlier Bell (1980 and 1983), Rahuel et al. (1989) and Holly and Rahuel (1990a) incorporated the spatial lag effects of bed load transport into their models by adopting Equation **(1)**. Meanwhile in Phillips (1984 and 1989) represented the spatial lag effects by directly bounding analysis for the sediment mass balance and analysis for the spatial lag effect of bed load transport and then solved them simultaneously. Equation **(1)** is adopted in the present model and is solved it. However, a series of comparison tests to assess which formulation gives more advantages to represent the spatial

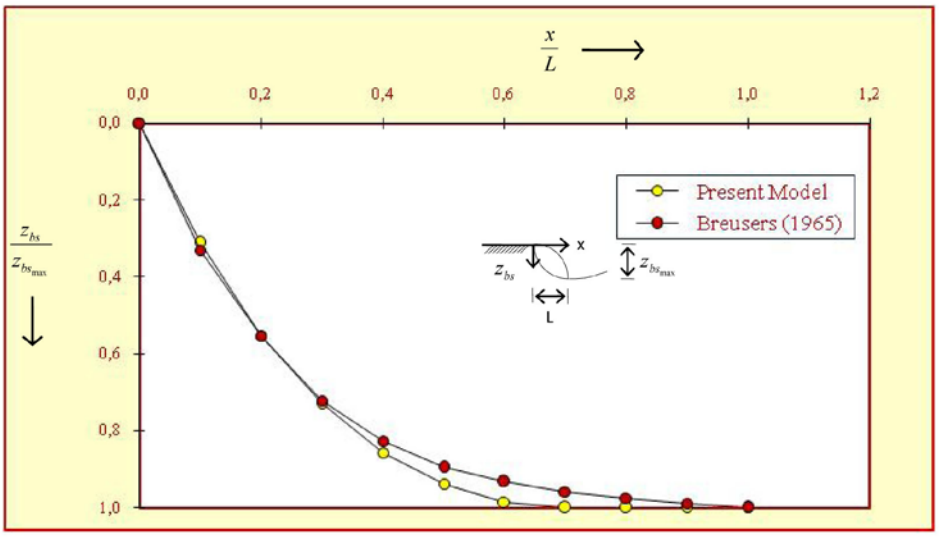

Figure 4 Scour hole profile in the separation zone

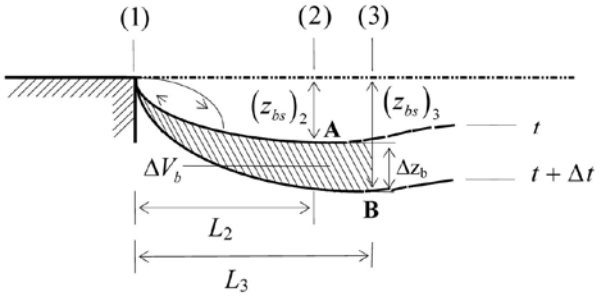

Figure 5 Diagram of the upstream bed load boundary scheme

lag effect is still needed and is carried out in the present study. For this purpose, both formulations are coded and tested in the present model tests. Moreover, the carried out tests are organized based on the following scenarios:

1) Test Series 1 is carried out to assess the model capability to simulate the experiments of Bell where the spatial lag effects of bed load are present. The assessment is undertaken by comparing the flume data to the model predictions on:

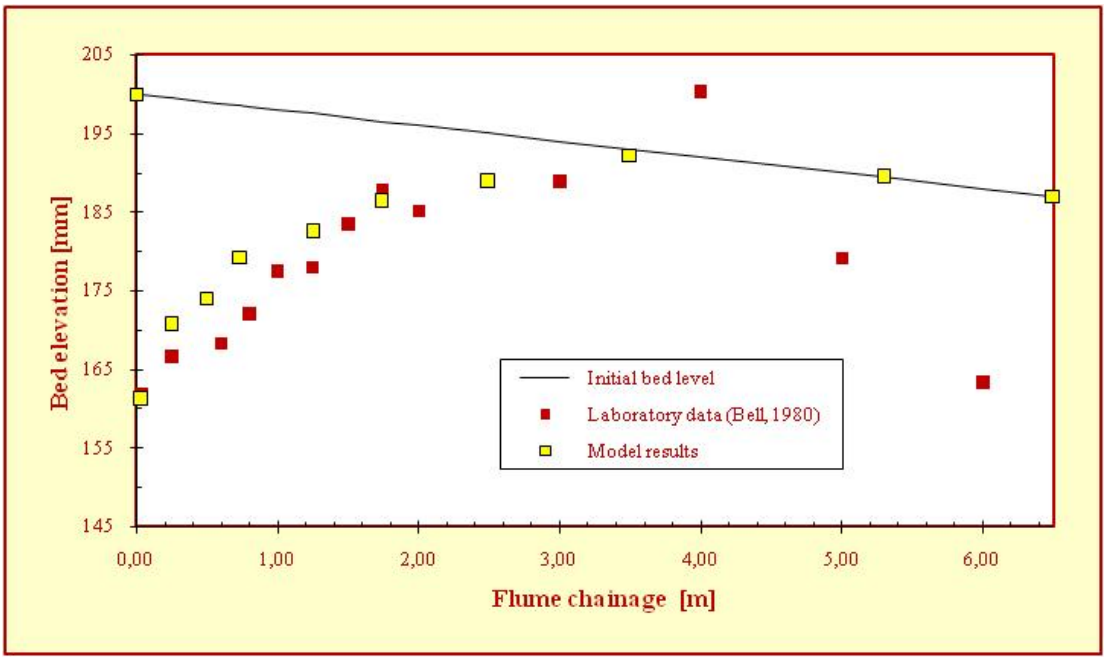

Figure 6 Effects of incorporating the spatial lag effects of bed load transport on bed level changes at t = 1800 s for the test Series 1, Numerical data: Δt = 0.15 s, Cr_w = 0.01 - 0.85, Cr_s = 1.6 E-6 - 1.25 E-4 and Fr = 0.60.

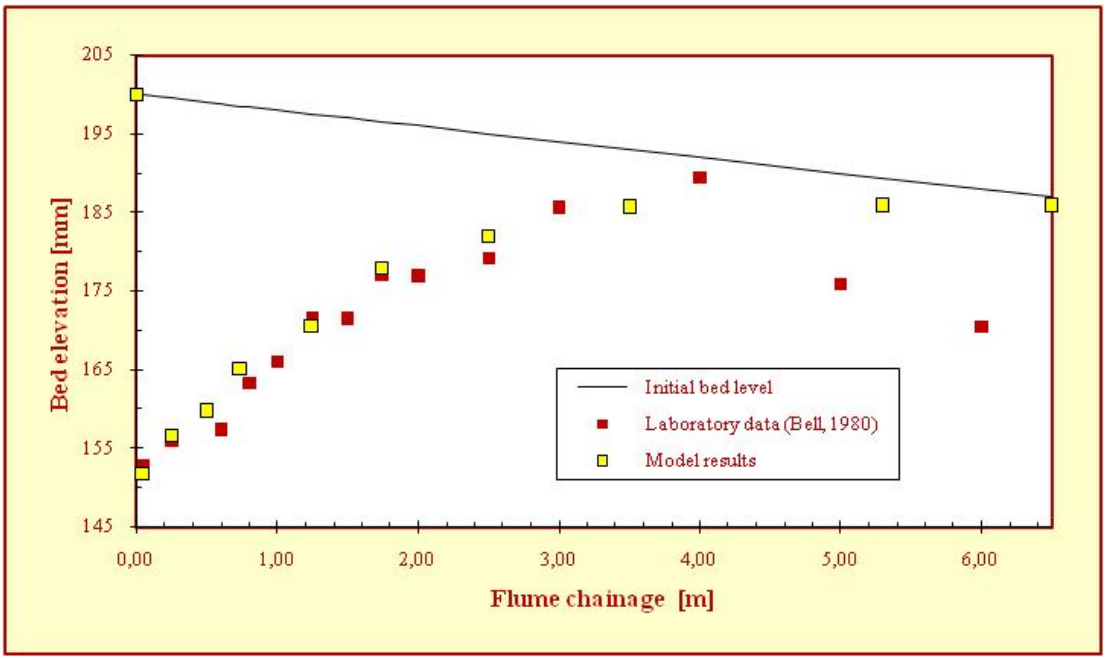

Figure 7 Effects of incorporating the spatial lag effects of bed load transport on bed level changes at t = 3600 s for the test Series 1, Numerical data: Δt = 0.15 s, Cr_w = 0.01 - 0.85, Cr_s = 1.6 E-6 - 1.25 E-4 and Fr = 0.60.

a) the bed level evolution along the flume at t = 1800 and 3600 seconds, and
b) the time variation of bed load transport rate at chainages x = 0.74, 1.74, 3.50 and 5.30 m.

2) Test Series 2, the two discussed above model formulations are compared to simulate the experiments of Bell. Evaluation is carried out based on their predictions on:
a) the bed level evolution along the flume at t = 1800 seconds, and
b) the time variation of bed load transport rate at chainages x = 0.74 m.

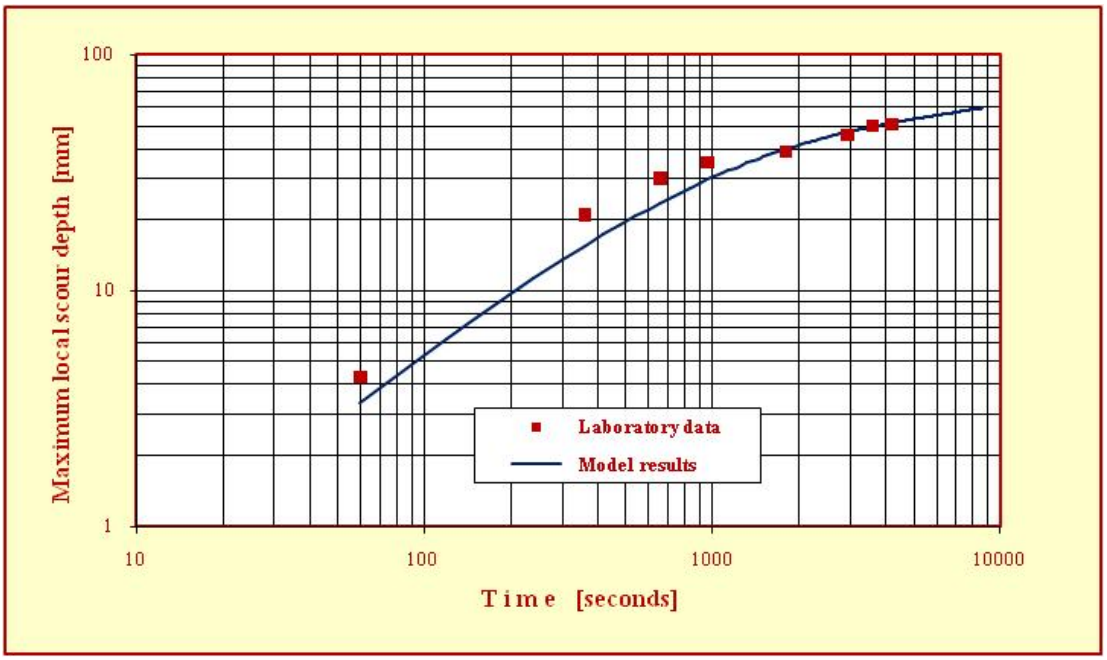

Figure 8 Time variations of the predicted local maximum depth given by the upstream boundary module for the test Series 1, Numerical data: Δt = 0.15 s, Cr_w = 0.01 - 0.85, Cr_s = 1.6 *E*-6 - 1.25 *E*-4 and Fr = 0.60.

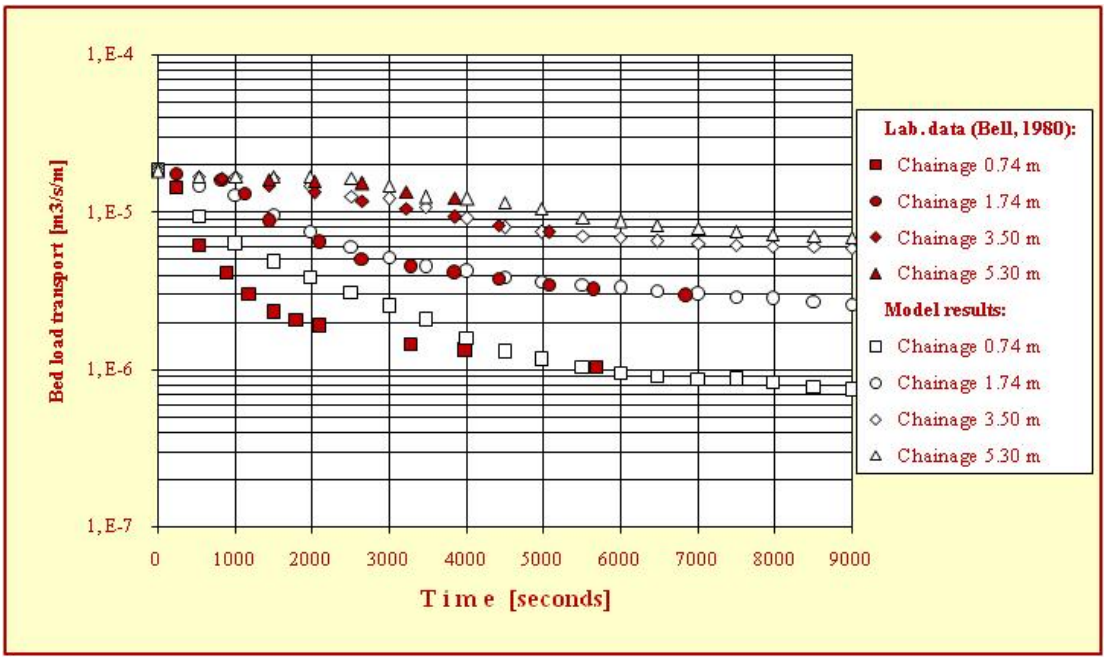

Figure 9 Effects of incorporating the spatial lag effects of bed load transport on time variation of bed load transport rate at various chainages for the test Series 1, Numerical data: Δt = 0.15 s, Cr_w = 0.01 - 0.85, Cr_s = 1.6 *E*-6 - 1.25 *E*-4 and Fr = 0.60.

The data of chainage x = 0.74 m is selected for this comparison test due to the relatively rapid time variations in the morphological processes.

3) Test Series 3, the sensitivity test to the taken space steps is carried out by using the present model with equation **(1)** only. The evaluation is based on the same criteria used in the test Series 2.

5) Model results and discussion

The flume schematization is discussed in Sub-section 2. The 24 non-uniform elements with space steps, Δx = 0.25 m - 20.0 m are used to represent the flume. While smaller space steps are used to resolve the scour hole region, the space steps are gradually enlarged in the downstream direction. A small time step, Δt = 0.15 seconds, is applied to the achieve numerical convergence. Based on a flow of q = 0.159 $m^3/s/m$, a water depth of h = 0.20 m and the aforementioned space and time steps, the following parameters can be derived:

1) the Froude number is $\boldsymbol{Fr}$ = 0.6,
2) the Courant numbers for water are $\boldsymbol{Cr}_w$ = 0.01 - 0.85, and
3) the Courant numbers for the sediment are $\boldsymbol{Cr}_s$ = 1.6 x 10^{-6} - 1.25 x 10^{-4}.

The results of the test Series 1 for the bed level evolution and the predicted sediment transport are presented in Figures 6 to 9. Figures 6 and 7 contain the comparison results of the predicted bed profiles and the measured bed profiles at t = 1800 seconds and t = 3600 seconds respectively. Overall, the agreement between the predicted and measured bed profiles is good. In general the predicted bed profiles are slightly higher than the measured data. This is understandable considering that the measured data refers to the centerline values, while the model is only capable of predicting the mean bed profile. Furthermore, a significant discrepancy can be noted at the downstream end of the scour hole. This discrepancy is caused by the presence of bed forms at the downstream of the scour hole region of the flume. The geometry data of the measured bed forms was length, λ = 2 m and height, H = 20 mm (Bell, 1980). The present model is unable to model individual bed forms.

Figure 8 contains the predicted maximum scour depth due to the presence of a fluid vortex at the downstream end of the fixed bed. The scour depth is predicted by using the upstream boundary module as discussed in Sub-section 3. It is evident in Figure 8 that the agreement between the predicted and the measured time variation of the maximum scour depth is good.

The predicted and measured bed load transport rates at several chainages within the developing scour hole are compared in Figure 9. The agreements between the measured and predicted sediment transport rate at chainages of 1.74 m, 3.50 m and 5.30 m are good, while the agreement at chainage x = 0.74 m is relatively poor. The maximum discrepancy at chainage x = 0.74 m is about 80%, while the noted maximum discrepancies at the other chainages are less than 15%. It is not clear why the error at chainage x = 0.74 m is approximately five times higher than those noted at the other chainages. The discrepancy at chainage x = 0.74 m is probably caused by the difficulties encountered when measuring sediment transport rate at this very short distance downstream of the fixed bed.

In this region a zone of separation occurred, a fluid vortex and a scoured hole formed. These relatively rapid time variations in the morphological processes may cause inaccuracy in the collected data from this region (Bell, 1980). This reason is supported by fact that a better agreement occurs between the measured and predicted data at time level Δt > 3000 seconds. At this time level and after, as can be seen in Figure 8, the rate of local scouring is decreasing. In these conditions, it is presumed that the bed load transport rate could be easier to be collected and measured. Therefore, a better accuracy of the collected data is achieved. The results of the test Series 2 for the bed level evolution and the predicted sediment transport rate are presented in Figures 10 and 11. The results in Figure 11 refer to the predicted sediment transport rate at chainage x = 0.74 m. The main conclusion from these results is that the difference between the results from the two formulations for the spatial lag effects of bed load transport is insignificant when compared to the laboratory data. Therefore based on these test results the simplest formulation, ie. as determined by Equations **(1)** and **(2)**, are to be preferred and adopted in the present model.

Sensitivity tests on the space steps are carried out in the test Series 3. For this purpose, the first thirteen elements are reduced by a half, giving rise to thirty six linear elements in total. The layout of the first 25 nodes are presented in Figure 12. The evaluation is only carried out within a region where the relatively rapid time variations in the morphological processes take place.

Figures 13 and 14 contain the results of test Series 3 for the predicted bed level evolution and bed load transport rate. To achieve the numerical convergence requirement, time step of

Δt = 0.05 seconds was taken in the model with reduced space steps. It is evident in Figures 13 and 14 that refining the space steps does not significantly affect the model results. Although there is a slight improvement, ie. about 10%, in the predicted rate of bed load transport when using the smaller space steps, this improvement requires a significant longer computation time.

Bell (1980) noted in his experiments that the clear water inflow required a significant distance, often as long as a half the length of the flume, to take on its bed load transport capacity.

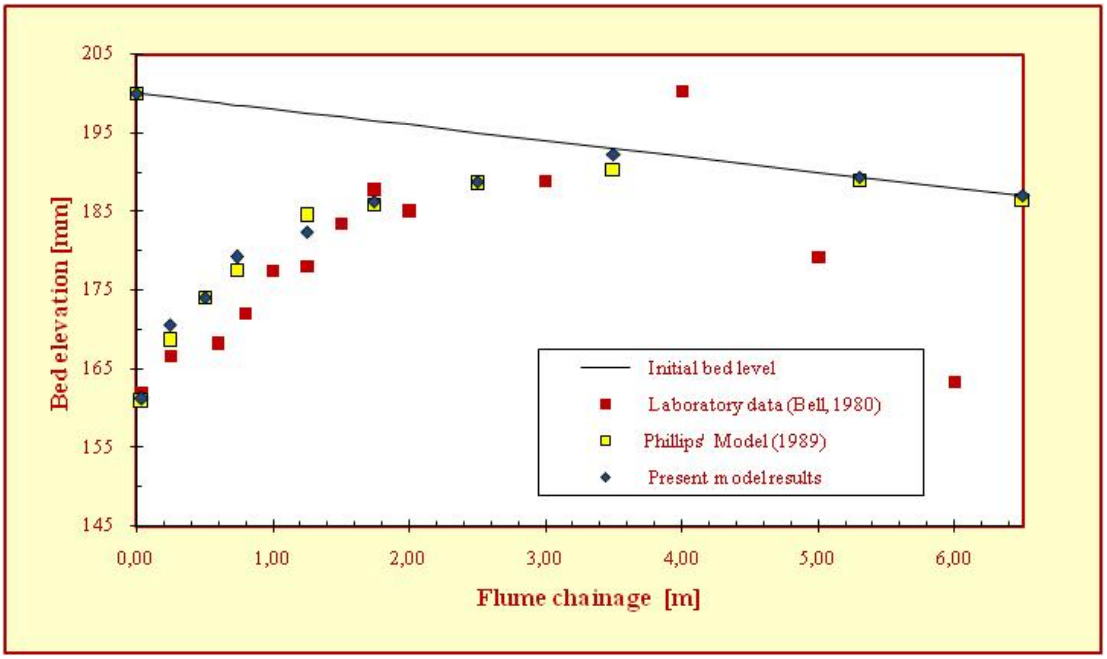

Figure 10 Effects of incorporating the spatial lag effects of bed load transport on bed level changes at t = 1800 s for the test Series 2, Numerical data: Δt = 0.15 s, Cr_w = 0.01 - 0.85, Cr_s = 1.6 *E*-6 - 1.25 *E*-4 and *Fr* = 0.60.

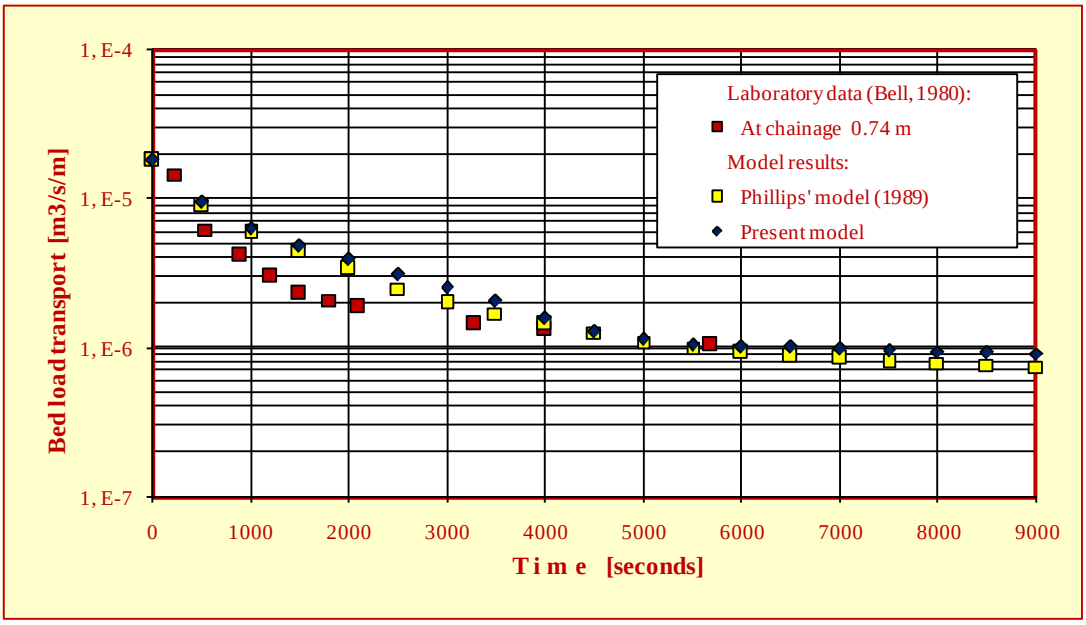

Figure 11 Effects of incorporating the spatial lag effects of bed load transport on time variation of bed load transport rate at chainage *x* = 0.74 m for the test Series 2, Numerical data: Δt = 0.15 s, Cr_w = 0.01 - 0.85, Cr_s = 1.6 *E*-6 - 1.25 *E*-4 and *Fr* = 0.60.

This data causes the following contradictions:

1) To appropriately simulate the experiments of Bell, the space steps must be selected finer than the adaptation length of bed load transport.
2) A restriction in the one-dimensional morphological models is that the space steps must be selected wider than the adaptation length required by the flow to reach its transport capacity (de Vries, 1987 and Cunge et al., 1980).

However, it is evident from the test results that the adoption of the spatial lag effect of bed load scheme solves those contradictions and enables the present model to adequately simulate the experiments of Bell.

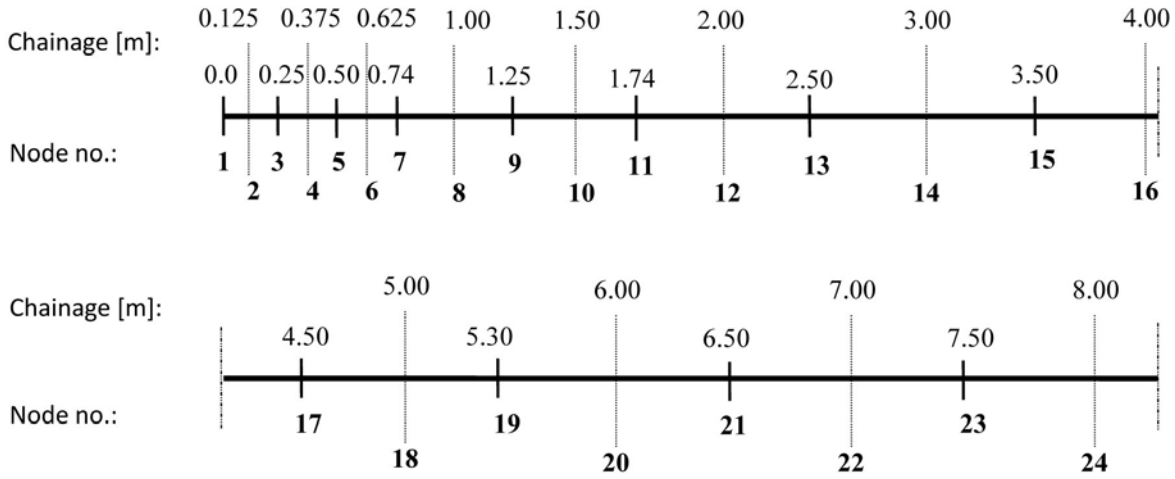

Figure 12 Chainage the along flume and refined elements configuration of the numerical model

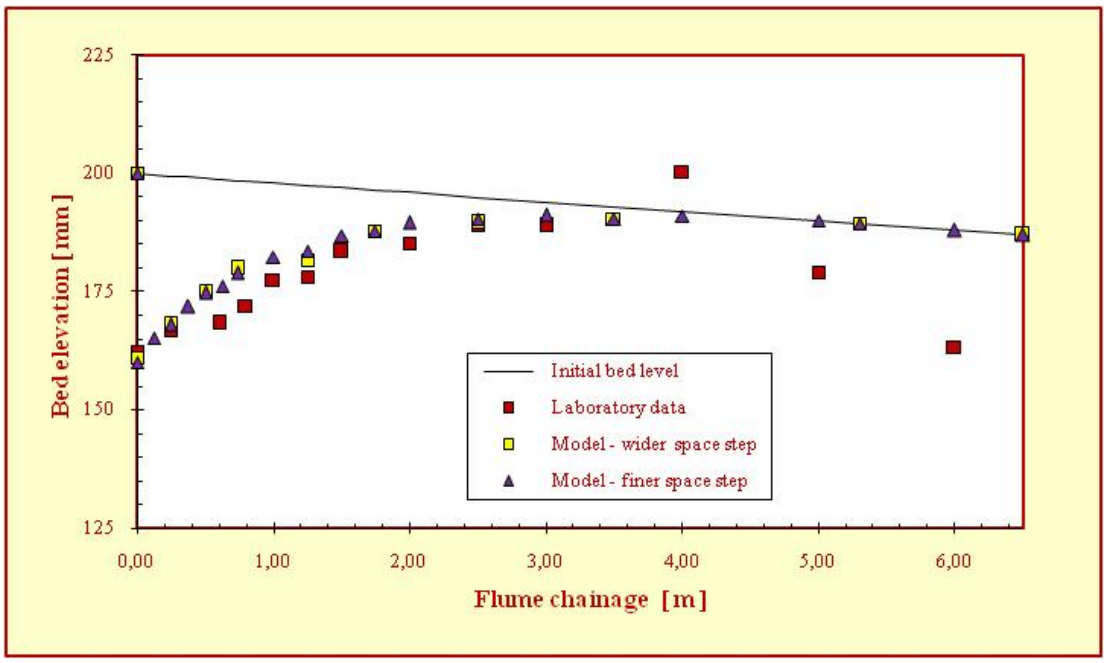

Figure 13 Sensitivity of the predicted bed elevation to space steps for the test Series 3, bed level changes at t = 1800 seconds, with data:

- Model using wider space steps: Δt = 0.15 s, Cr_w = 0.85, Cr_s = 1.25 E-4 and Fr = 0.60,
- Model using finer space steps: Δt = 0.05 s, Cr_w = 0.60, Cr_s = 0.85 E-4 and Fr = 0.60.

6) Summary of the test results on the bed level changes

Series of tests have been carried out to verify the capability of the sub-model for predicting bed level changes. The carried out tests consider bed load transport rate under steady flow but the sediment transport rates are not equal to the transport capacity. The model is well capable to predict the bed level changes. It is concluded from a comparison with scour hole evolution downstream of a fixed bed. Aside from the results of the chainage which is located in the flow vortex zone, the present model predictions of the bed load transport rate are agree with the flume data of Bell (1980).

CONCLUSIONS

1) The present study has resulted in the Bed Load Sub-model that has capabilities to analyze bed load sediment transport capacity under unsteady flow conditions by including the spatial lag effects of the alluvial reach.
2) The performance and robustness of the sub-model have been evaluated in simulating the local scouring pattern and depth of alluvial reach downstream of a sediment barrier. Its prediction has been verified by laboratory data and shows its good agreement.
3) The Bed Load Sediment Transport sub-model allows the designed riverine fully coupled finite element model with sediment transport sub-processes to cope with the following conditions:
   a) an imposed non-equilibrium sediment boundary conditions,
   b) situations where the space steps need to be taken shorter than the adaptation length required by the flow to reach its transport capacity, and
   c) condition where the actual sediment transport rate is different from the flow transport capacity.

REFERENCES

Bell, Robert G. (1980). Non-equilibrium bedload transport by steady and non-steady flows. University of Canterbury, Christchurch, New Zealand, PhD Thesis.

Bell, R.G. and A.J. Sutherland (1983). Non equilibrium of bed load transport by steady flow. Journal of Hydraulic Research, IAHR, Vol 109, No. 3, pp. 351-367.

Breusers, H.N.C. (1965). Conformity and time scale in two-dimensional local scour. Publication No. 40, Delft Hydraulics Laboratory.

Cunge, J.A., F.M. Holly Jr. and A. Verwey (1980). Practical aspect of computational river hydraulics. Pitman Publishing, Boston.

Einstein, H.A. (1950). The bed-load function for sediment transportation in open channel flow. Technical Bulletin No. 1026, U. S. Department of Agriculture, Washington, D. C.

Holly, F.M. Jr. and J.L. Rahuel (1990a). New numerical/physical framework for mobile bed modelling, Part I Numerical and physical principles. Journal of Hydraulic Research, IAHR, Vol. 28, No. 4, pp. 401- 416.

Johnson, J.W. (1942). The importance of side-wall friction in bed load investigations. Civil Engineering, Vol. 12, No. 6, pp. 329-331.

Phillips, B.C. (1984). Spatial and temporal lag effects in bedload sediment transport - Civil Engineering Research Report No. 84-10 - Reprint of PhD Thesis, Department of Civil Engineering, University of Canterbury.

Phillips, B. C. and A. J. Sutherland (1989). Spatial lag effects in bed load sediment transport. Journal of Hydraulic Research, IAHR, Vol. 27, No. 1, pp. 115-133.

Phillips, B. C. and A. J. Sutherland (1990). Temporal lag effects in bed load sediment transport. Journal of Hydraulic Research, IAHR, Vol. 28, No. 1, pp. 5-23.

Rijn, L.C. van (1984b). Sediment pick-up functions. Journal of Hydraulic Engineering, ASCE, Vol. 110, No. 10, pp. 1494-1502.

Singh, A.K., Kothyari, U.C. and Rangga Raju, K.G. (2004). Rapidly varying flows in alluvial rivers. Journal of Hydraulic Research, Vol. 42, No. 5, pp. 473-486.

Vanoni, V.A. and N.H. Brooks (1957). Laboratory studies of roughness and suspended load of alluvial streams. Sedimentation Laboratory Report No. E68, California Institute of Technology, Pasadena, California.

Vries, M. de (1965). Considerations about non-steady bedload transport in open channels. Proceeding. of 11th Congress, IAHR, Leningrad, Vol. 3, Paper 3.8.

Vries, M. de (1987). Morphological computations - Lecture Notes. Delft University of Technology, Delft.

Yalin, M.S. (1977). On the physical modelling of dunes. Proceedings of XVIIth Congress, IAHR, Baden-Baden, Vol. 1, Paper A4, pp. 25-32.

Yiniarti, E.K. (2008). Penelitian karakteristik blok beton terkunci Balok Kaki 6 dan penerapan untuk pengendalian gerusan local di Bendung Gerak Pamarayan. Pusat Litbang Sumber Daya Air.